Broadside Gain Enhancement of Wideband Monopole Circular Shaped Antenna Using FSS for Sub-6 GHz Applications

Tamara Zuhair Fadhil[1,2], Noor Asniza Murad[1], and Mohamad Rijal Hamid[1]

***Abstract*—This paper introduces a wideband circular patch antenna designed with a frequency selective surface (FSS) for sub-6 GHz applications. The proposed antenna features a monopole circular-shaped patch with a partial ground plane, delivering an omnidirectional radiation pattern in the azimuth plane, resulting in relatively uniform gain in all directions. An FSS metamaterial enhances the antenna's gain and improves the broadside radiation pattern. The design incorporates three inner circular patches connected to the main patch. The FSS utilizes hybrid square/circle loop-based unit cells. The antenna and FSS are simulated using CST software and subsequently fabricated on an FR-4 substrate. The measured results demonstrate an impedance bandwidth of 1.6 GHz with a peak gain of 5.4 dB at 3.5 GHz. The omnidirectional radiation pattern is converted into a directional one by placing a reflector FSS as a bottom substrate layer. The overall structure size is compact, measuring (0.34λ0 × 0.27λ0 × 0.016λ0), where λ0 is the free-space wavelength corresponding to the lowest resonant frequency within the operational bandwidth. This design achieves significant antenna size reduction and is well-suited for future sub-6 GHz applications.**

***Index Terms*—Circular patch antenna, FSS, Sub-6 GHz, impedance bandwidth, broadside radiation pattern.**

I. INTRODUCTION

A THE MAJOR FOCUS IN RECENT YEARS HAS BEEN ANTENNA FRAMEWORKS OPERATING AT SUB-6 GHZ FREQUENCIES, WHICH ARE required to provide high gain and broadband performance in a compact package for wireless and mobile applications. Such antennas must feature a compact design, directional beams, exceptional radiation efficiency, and broader bandwidth [1–3]. Consequently, diverse types of planar and non-planar antennas have also been invented [4,5]. Unfortunately, such antennas have limited bandwidth and low peak gain [5,6]. At the same time, a monopole antenna has the disadvantage of low gain; reliance on the presence of the ground plane and partial ground plane significantly affects the antenna's asymmetrical radiation pattern. This, in turn, leads to uneven coverage and reduced performance in specific areas due to variations in gain and coverage characteristics. Different antennas with different shape implementations are proposed to overcome these problems. Shapes such as rectangular, circular, curved, and elliptical are presented with a partial ground plane [7,8]. [9] proposes a curved slot monopole antenna with a partial ground plane for wideband applications with an operating band 3 up to 12 GHz. Another shape of the elliptical ring antenna is presented in [10] for compact size and wideband properties. However, these designs suffer from low peak gain for LTE2600, Wi-Fi, WLAN, and UWB applications. Circular monopole antennas have advantages over other shapes due to their flexibility and wideband properties [11]. A novel configuration for a multi-frequency parasitic hat microstrip antenna is introduced for diverse communication needs. This innovative antenna design incorporates defected ground structure and microstrip structure techniques to enhance overall antenna performance [12]. Different methods and approaches are introduced to increase the gain and reduce the back lobe radiation of the circular patch antenna [13]. One of the essential methods is the introduction of FSS with single-layer and double-layer reflectors [13]. The works in [13] and [14] achieved a good gain enhancement with an impedance bandwidth of more than 1 GHz. However, the size of FSS used in these designs is still undesirable for sub-6 GHz applications. Recently, a single-layer FSS reflector has been proposed with a square circular-shaped monopole antenna [15]. Another FSS single-layer substrate is implemented with a planar antenna introduced in [16]. The FSS superstrate markedly improves the achieved antenna gain, boosting it by up to 5.22 dB within the UWB frequency range. A bandwidth enhancement of 50% with a gain of 5.1 dB is achieved in this design. Novel microstrip antennas with FSS using SRR unit cells are introduced in [17]. The FSS is implemented with a double layer's square loop-based unit cell. The antenna achieved a gain enhancement of 5 dB. However, the size of the FSS in both designs was quite massive, with a narrow bandwidth of 150 MHz. This paper presents a developed monopole circular patch antenna integrated with three inner circular patches for compact size and wideband properties. Then, a hybrid square/circle loop-based FSS metamaterial is designed to enhance the gain and broadside radiation pattern. The proposed antenna with FSS aims to acquire a wideband, compact size, and high efficiency. The antenna is intended to have an impedance bandwidth more significant than 1 GHz. The increased value should be more than 5 dB. A FR-4 substrate of 1.6 mm is used to fabricate the suggested antenna, including the FSS. This paper is organized as follows: Section 2 introduces the antenna design methods and the FSS. Section 3 reports the obtained results for the proposed designs, and section 4 summarizes the findings.

[1]Advanced RF and Microwave Research Group (ARFMRG), Faculty of Engineering, School of Electrical Engineering, Universiti Teknologi Malaysia (UTM), Johor 81310, Malaysia.

[2] University of Information Technology and Communications, Baghdad, Iraq, (E-mail: tamara@graduate.utm.my).

DOI: 10.36244/ICJ.2024.3.8

II. DESIGN OF THE CIRCULAR PATCH ANTENNA AND FSS

A circular patch antenna and FSS metasurface are designed based on the agreement of three circular patch elements and hybrid square/circle ring resonators (SRR/CRR) unit cells with parameters L_0= 7.15 mm square length, radius of inner ring *Rin* =5.06 mm, and width s=0.6 mm to enhance the gain and enhance the broadside radiation pattern. The designs are implemented with an affordable FR-4 substrate with a thickness h= 1.6 mm and relative permittivity εr =4.3. The following sub-sections discuss the design methods for both the antenna and the FSS metasurface.

A. Design of circular monopole antenna

Fig. 1 (a) illustrates the proposed antenna structure and design steps. It starts with a circular patch antenna design from extended to partial ground planes. A circular patch with an inner radius of R is designed based on the following formulas [18]:

$$R = \frac{R_{eff}}{\left(1+\frac{2h}{\pi\varepsilon_r R_{eff}}\left[\ln\left(\frac{1.57R_{eff}}{h}\right)+1.78\right]\right)^{0.5}} \quad (1)$$

$$R_{eff} = \frac{8.79\times10^9}{f_r\sqrt{\varepsilon_r}} \quad (2)$$

Where R_{eff} is the effective radius, and f_r is the desired resonant frequency.

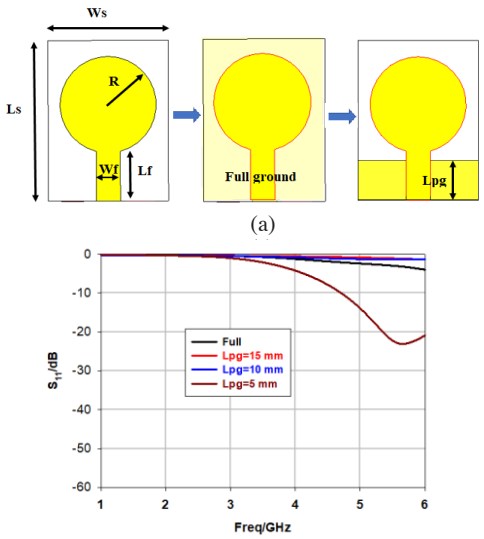

Fig. 1. (a) The circular antenna structure. (b) Return loss parametric study.

A parametric study is performed using CST microwave software to analyze the performance of the return loss (S11) variation concerning the full and partial ground length. Fig. 1 (b) shows the return loss responses over the sub-6 GHz band. It can be noticed from Fig. 1(b) that the length of partial ground plays a crucial role in the frequency resonation. As the length of partial ground reduces, the resonant frequency shifts to the lower edge close to 4.7 GHz. In summary, if the ground plane length is shorter than one-quarter of the wavelength, it will significantly influence the antenna's resonant frequency in the horizontal (X-axis) and vertical (Y-axis) dimensions.

Removing the partial ground plane on the current surface contributes to E-plane diffraction. As the length of the partial ground plane increases, the E-plane in the back lobe radiation rises. This way, the main and the back lobe have minimal surface current at E-plane edge diffraction. Hence, the initial value of partial ground length is 5 mm, with *R* being 7.5 mm at the desired frequency of 3.5 GHz. An inner circular slot is inserted in the center of the circular patch antenna, including a 2.8 mm diameter, as shown in Fig. 2 (a).

The effect of the slot radius has a crucial role in the bandwidth and size performance of the circular antenna. The circular patch antenna size decreases with the increase of the slot radius, which reduces the overall size of the antenna. Additionally, this insertion of the circular slot increases the impedance bandwidth and shifts the frequency to the lower band of 2.7 GHz. This is illustrated in Fig. 2 (b). The return loss is enhanced by a peak value of -25 dB at 3.1 GHz with a frequency shift to the lower band below 3.5 GHz with a -25 dB peak value at 3.1 GHz.

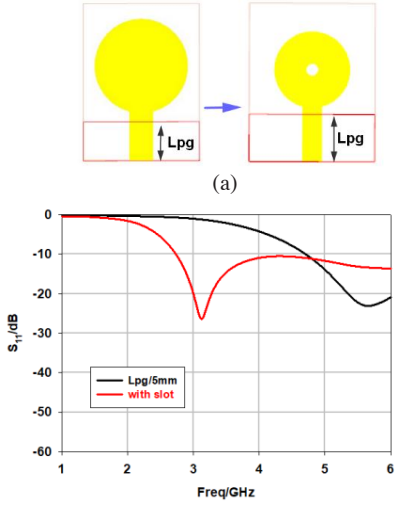

Fig. 2. (a) Modified antenna with the center slot. (b) Return loss responses.

Inserting a parasitic element can result in a smaller overall antenna structure. The parasitic element can assist in achieving resonance and optimizing radiation performance characteristics. This leads to a reduced antenna physical size, consequently yielding a more compact antenna.

As a result, the proposed antenna is developed by adding three inner circular patches at the corners of the original patch, as illustrated in Fig. 3 (a). Each of the three circular patches has the same radius value, which can be found by the following formula:

$$R_1 = 0.3\ R \quad (3)$$

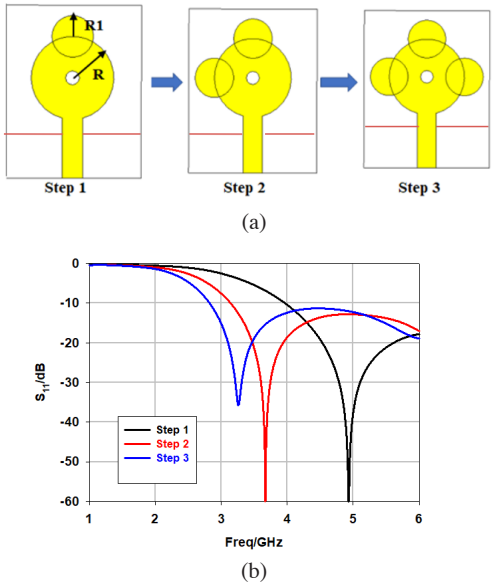

Fig. 3. (a) Design steps of the proposed antenna. (b) Return loss responses.

Fig. 3 (b) plots the variation of the proposed antenna's return loss. As each circular patch is inserted, the resonant frequency shifts to the lower frequency band from 4 GHz toward the frequency band of 2.7 GHz. The impedance bandwidth is expanded to more than 3 GHz as all three patches are inserted on the original patch, which indicates that the fractional bandwidth (FBW) of the proposed antennas is improved by 85.5% compared to the original antenna FWB of 50%.

Therefore, the final dimensions of the proposed antenna are as follows: (*Ls*=33 mm, *Ws*=26.4 mm, *Wf*=3.112mm, *Lf*=11.47 mm, *Lpg* =9.9 mm, *R*=7.48 mm, and *R1*=2.6 mm).

B. FSS configuration with the antenna

Fig. 4 (a) shows the proposed configuration of the antenna with an FSS substrate. The FSS substrate works as a reflector to emphasize the broadside radiation and increase the antenna's main beam (gain). The FSS configurations consist of a 3 × 4 unit cells array. The FSS substrate is placed below the antenna substrate, facing the antenna's partial ground plane. FSS is a spatial resonance structure with various responses to EM waves at specific frequencies. Hence, this paper uses hybrid square/circle loop-based FSS as a partial reflection surface (PRS) at 3.5 GHz. The square/circle unit cell acts as a parallel *LC* resonance, considering an open circuit at the desired frequency. At the desired frequency of 3.5 GHz, the air gap between the two substrates is chosen to be equal to (λ_g/4), where λ_g is the guided wavelength. For this purpose, wideband property is achieved with gain enhancement. In that matter, the radiation is mainly reflected in one direction, eliminating the original antenna radiation by having a phase difference of 180°. Two conditions are required to eliminate the reflected and incident angles to achieve that. These conditions are realized with the following [19]:

$$2\pi \frac{2d}{\lambda_g} + \varphi_r = (2n+1)\,\pi \quad (4)$$

$$\pi + 2\pi \frac{2d}{\lambda_g} + \varphi_r = 2n\pi \quad (n = 0, 1, 2, \ldots) \quad (5)$$

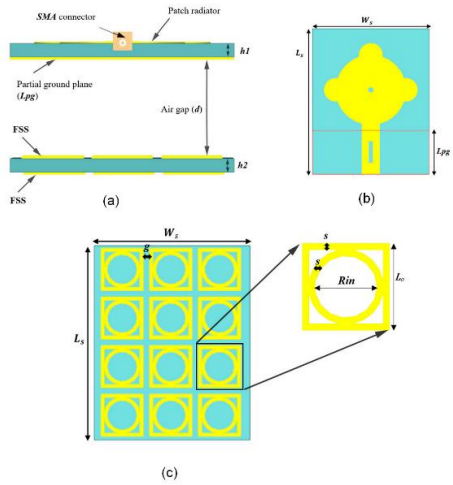

Fig. 4. (a) Antenna with FSS layers configuration, (b) Antenna layer, (c) FSS layer.

Therefore, a parametric simulation study is achieved regarding the distance (*d*) between the antenna substrate and the FSS substrate, as illustrated in Fig. 5 (a) and (b), respectively. Fig. 5 (a) shows the return loss variations with varied values of d. In such cases, the distance between the substrates increases, and the return loss value rises with shifting to a higher band above 3.5 GHz. However, at d= 11.5 mm, the return loss is -18 dB at the desired frequency of 3.5 GHz. Making a slot cut with a dimension of $L \times W$ =5 ×1 mm^2 inside the antenna's feedline will enhance the return loss to -58 dB. Then, the impedance bandwidth of 2 GHz with FBW of 57% is achieved.

Similarly, the antenna radiation pattern (with FSS applied) with different values of air-gap distance is plotted in Fig. 5 (b). At the optimized value of *d*= 12 mm, the primary lobe radiation is increased to 5.6 dB compared to the reference antenna of 2.25 dB. Moreover, the antenna's performance is evaluated when a Perfect Electric Conductor (PEC) is used in place of the FSS layer at the optimized distance. This extra evaluation is considered an additional simulation for comparative analysis. The PEC layer position can impact the antenna's resonance and S_{11} performance. The separation distance of air between the layers may generate capacitance between the PEC layer and the antenna. The effect of capacitance may slightly raise the effective electrical length of the antenna, causing the resonance frequency to shift downwards, as depicted in Fig. 5 (a). This PEC layer serves as the antenna's reflector. Nonetheless, a limitation of the PEC layer arises from generating a reflected wave that exhibits a 180-degree phase shift relative to the source wave, as illustrated in Fig. 5 (b).

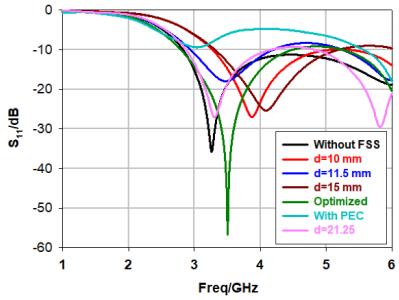

(a)

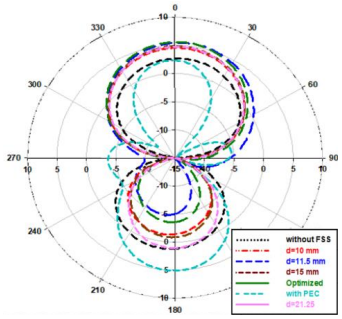

(b)

Fig. 5. (a) Parametric study on return loss regarding *d*. (b) Parametric study on radiation pattern regarding *d* at E plane.

III. Results and Discussion

The antenna and FSS prototypes were fabricated and measured, as depicted in the following figures. Figure 6(a) and (b) show the top and bottom sides of the fabricated antenna with FSS layers, respectively. Figure 7 illustrates the return loss and radiation pattern measurement. The antenna, with and without the FSS, was measured using a Rohde & Schwarz ZVL Vector Network Analyzer (VNA), which operates over a frequency range of 9 kHz to 13.6 GHz. The VNA was calibrated using a standard calibration kit to ensure measurement accuracy. However, it is essential to note that a cable loss of 2 dB post-calibration could affect the return loss measurement process, and this loss should be considered.

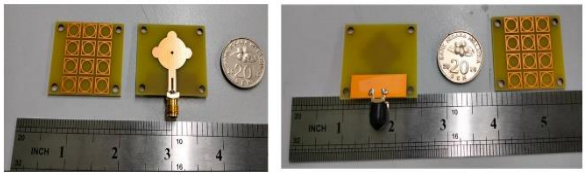

Fig. 6: (a) Top and (b) bottom side of fabricated antenna with FSS layers.

The radiation pattern measurements were performed inside an anechoic chamber, which has dimensions of 3.2 x 4.6 x 2.8 meters. The chamber is equipped with pyramidal microwave absorbers and optimized for measurements in the 100 MHz to 18 GHz frequency range. A standard horn antenna was used as the signal transmitter, while the antenna under test (AUT) received the signal, and a spectrum analyzer measured the signal magnitude. This process was conducted twice: once with the antenna only and once with the FSS placed below the antenna. The results were obtained from return loss (S11) and the radiation patterns (Theta vs. dB).

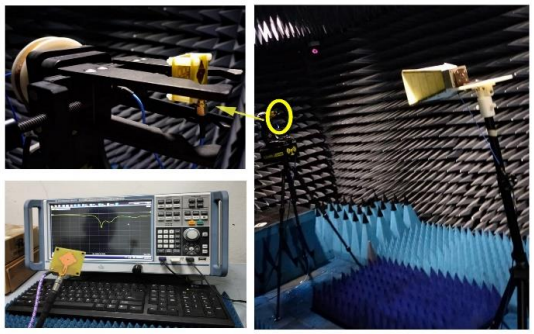

Fig. 7. Measurement components setup.

A. *Antenna without FSS*

The measured and simulated return loss (S_{11}) of the antenna without FSS are present in Fig. 8 (a). With a measured bandwidth between 3.1 and 5.7 GHz, the observed value is -33 dB as contrasted to the simulated value of -35 dB. Hence, the proposed antenna has an optimized return loss and bandwidth. The measured radiation pattern is plotted against the simulated one in Fig. 8 (b). The maximum gain of 1.97 dB is obtained in the front-back ratio, which is less than 0.28 dB compared to the simulated radiation pattern of 2.25 dB. Fabrication errors and cable losses cause this loss in gain value.

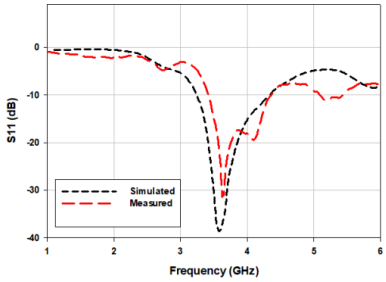

(a)

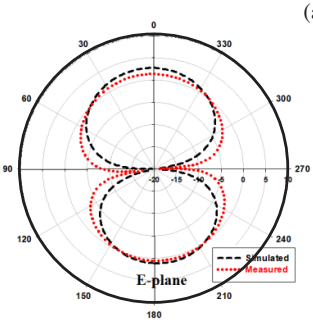

(b)

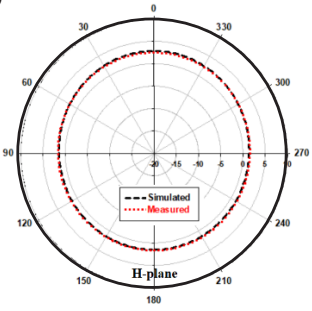

(c)

Fig. 8. Measured Antenna results. (a) Return loss. (b) Radiation pattern at E-plane (c) Radiation pattern at H-plane.

B. *Antenna with FSS*

The comparison between the antenna's simulated and measured return loss with FSS is illustrated in Fig. 9 (a). The measured S_{11} is -32 dB as contrasted to the simulated one of -59 dB. The fractional bandwidth is around 67%, with a measured bandwidth range between 3 and 4.5 GHz. Hence, the proposed antenna with FSS has a wide bandwidth. The measured plane and H-plane radiation pattern with the simulated one is shown in Fig. 9 (b). The measured E-plane agreed well with simulated results as the main lobe value of 5.4 dB.

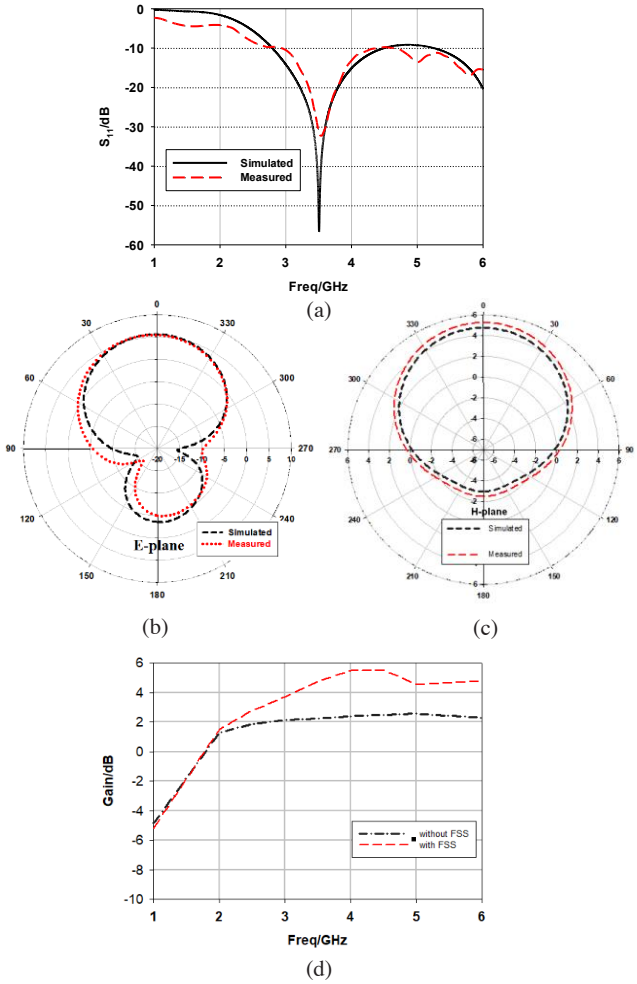

Fig. 9. Measured Antenna with FSS results. (a) Return loss (b) Radiation pattern E-plane (c) Radiation pattern H-plane (d) Broadside gain.

Similarly, the measured H-plane follows the same performance as the H-plane simulation. At 3.5 GHz, the measured gain is 5.4 dB compared to the simulated gain of 5.6 dB. The comparison of the measured gain of the antenna alone with the measured gain of the antenna with FSS is plotted in Fig. 9 (c). It is noticed that adding FSS with the antenna increased the gain by an additional 3 dB to the original antenna gain. Hence, it can be concluded that FSS improves the antenna gain and enhances the broadside radiation pattern.

Fig. 10 (a) and (b) show the current distribution and intensity of the circular patch antenna with FSS. It can be clearly noticed that a concentration and saturated current are distributed by the FSS array unit cells. This significantly improves the antenna's gain. Hence, Table I summarizes the results obtained by the antenna with and without FSS. Table II presents a comparison between this work and previous works related to the circular antenna and FSS. The proposed antenna with FSS is compared with the other designs in terms of frequency range, gain, and size. As a result, it is proven that the proposed antenna in this work has a good gain, appropriate bandwidth, and small size, and it achieved a significant broadside radiation pattern value.

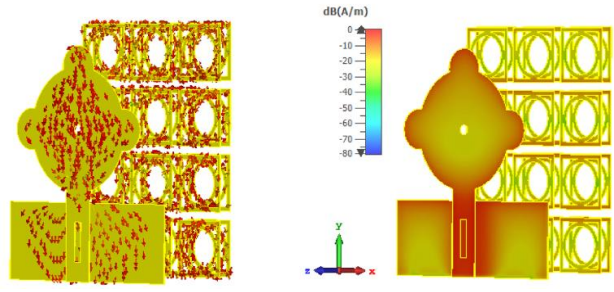

Fig. 10. (a) Surface current (b) current density distribution of the proposed antenna with (4 × 3) FSS at 3.5 GHz.

TABLE I
THE PERFORMANCE OF THE PROPOSED ANTENNA WITH FSS AT 3.5 GHZ.

Evaluation metrics	Antenna without FSS		Antenna with FSS	
Performance	Sim.	Mes.	Sim.	Mes.
Return loss S_{11}(dB)	-35	33	-59	-25
Bandwidth (GHz)	3	1.6	1.7	1.6
Gain (dB)	2.25	1.97	5.6	5.4

TABLE II
COMPARISON OF THIS WORK WITH RELATED OTHER ANTENNAS.

References	Frequency (GHz)	BW (GHz)	Gain (dB)	Backward radiation (dB)	Antenna Size (mm^2)	FSS size (mm^2)	Unit cell no
[17]	2.3 to 2.6	0.23	6.8	-0.82	75 × 75	54×65	5 × 5
[20]	2.9 to 9.1	8.85	7.8	-8	26×26	61×61	10×10
[21]	3-10	3	6.9	-6	16 × 22	52 × 62.5	6×5
[22]	2.82	6	4	-4	34×41	45×45	4×4
[23]	3-5.5	5.5	7	high	110×110	110 ×59	(9×15) + (5×6)
[24]	3.1–18.6	15.5	6.9	-5	16 × 22	52 × 62.5	6×5
[25]	3-14	10.8	4.5	high	30 x 30	62.5 x 62.5	6x6
[26]	3.3–4.2	12.39	6.2	high	29 × 23	50 x 50	5 x 5
This work	3 to 4.6	1.6	5.4	-9	36.4 × 36.4	30 × 26.4	4×3

Fig. 11 (a) presents the electric field distribution of the antenna with a partial ground plane and integrated frequency selective surface (FSS). The observed ring-shaped pattern, centered above the ground plane, indicates effective coupling and interaction between the FSS and the antenna, contributing to enhanced beam shaping and directivity.

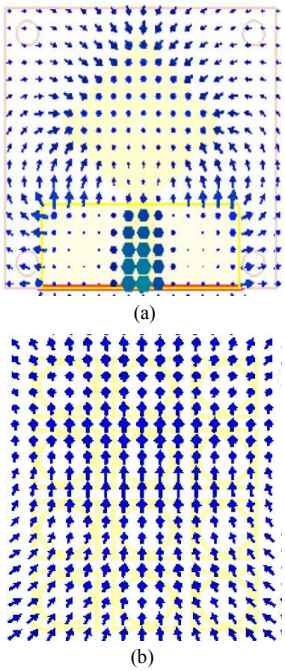

Fig. 11. Electric field distribution of the developed antenna at 3.5 GHz (a) antenna layer (b) FSS layer

Fig. 11 (b) illustrates the electric field distribution across the FSS, exhibiting a periodic and symmetrical pattern. This distribution suggests strong field confinement and efficient resonance within the FSS elements, which is crucial for controlling electromagnetic wave propagation and achieving the intended filtering effects.

IV. CONCLUSION

In this work, a designed wideband circular patch antenna with square/circle loop-based FSS is presented at 3.5 GHz. The circular antenna is implemented with three inner circular patches of transmission lines and a partial ground plane. Then, the gain and the broadside radiation pattern are enhanced using the designed FSS placed in the back of the antenna. The measured realization of the prototype is agreeable with the simulated results. At 3.5 GHz, prominent bandwidth, S-parameters, gain, and broadside radiation pattern performance are attained. With a fractional bandwidth of 67%, the antenna performs at the frequency range of 3 to 4.6 GHz. The antenna evolved to be compact and low-profile. For sub-6 GHz applications, the suggested antenna with FSS is applicable to be implemented with an antenna array.

ACKNOWLEDGMENT

This work is supported by Advanced RF and Microwave Research Group, Faculty of Electrical Engineering, Universiti Teknologi Malaysia (UTM), Johor Bahru. This work is funded by the Ministry of Higher Education under Fundamental Research Grant Scheme (Ref: FRGS/1/2021/TK0/UTM/02/62) and collaborative matching grant (Q.J130000.3023.04M33).

REFERENCES

[1] Y. He, S. Lv, L. Zhao, G. L. Huang, X. Chen, and W. Lin, "A Compact Dual-Band and Dual-Polarized Millimeter-Wave Beam Scanning Antenna Array for 5G Mobile Terminals," IEEE Access, vol. 9, pp. 109 042–109 052, 2021, DOI: 10.1109/ACCESS.2021.3100933.

[2] S. Islam, M. Zada, and H. Yoo, "Highly Compact Integrated Sub-6 GHz and Millimeter-Wave Band Antenna Array for 5G Smartphone Communications," IEEE Trans. Antennas Propag., 2022, DOI: 10.1109/TAP.2022.3209310.

[3] H. Almizan et al., "Novel metasurface based microstrip antenna design for gain enhancement RF harvesting," Infocommunications Journal, vol. 15, no. 1, pp. 2–8, 2023, DOI: 10.36244/ICJ.2023.1.1.

[4] N. S. Babu et al., "Dual-Band Circularly-Polarized EBG-Based Antenna for Wi-MAX/WLAN/ISM Band Applications," Wireless Pers. Commun., 2022, DOI: 10.1007/s11277-022-09951-0.

[5] T. Z. Fadhil et al., "A Beam-Split Metasurface Antenna for 5G Applications," IEEE Access, vol. 10, pp. 1162–1174, 2022, DOI: 10.1109/ACCESS.2021.3137324.

[6] A. Balanis, Antenna Theory, Analysis and Design, 4th ed., Wiley, 2016, ISBN 978-1-118-64206-1.

[7] Y. Alnaiemy and L. Nagy, "A novel UWB monopole antenna with reconfigurable band notch characteristics based on PIN diodes," Infocommunications Journal, vol. 13, no. 3, pp. 33–44, 2021, DOI: 10.36244/ICJ.2021.3.4.

[8] M. F. Ahmed et al., "A Novel Compact Dual Notch with High-Gain Multi-Layer Dielectric Resonator Antenna for Ultrawide-Band Applications," 2022.

[9] A. Ibrahim and M. F. Abo Sree, "UWB MIMO antenna with 4-element, compact size, high isolation and single band rejection for high-speed wireless networks," Wireless Networks, 2022, DOI: 10.1007/s11276-022-03019-4.

[10] S. A. Alassawi et al.,"Compact elliptic ring 2 × 2 and 4 × 4 MIMO-UWB antenna at 60 GHz for 5G mobile communications applications," Microsystem Technologies, vol. 28, no. 2, pp. 1151–1161, 2022, DOI: 10.1007/s00542-022-05383-9.

[11] S. Das, D. Mitra, and S. R. Bhadra Chaudhuri, "Fractal loaded circular patch antenna for super wide band operation in THz frequency region," Optik (Stuttgart), vol. 226, p. 165 528, 2021, DOI: 10.1016/j.ijleo.2020.165528.

[12] F. F. Ismail, M. A. El-Aasser, and N. H. Gad, "A Parasitic Hat for Microstrip Antenna Design Based on Defected Structures for Multiband Applications," ACES Journal, 2022, pp. 568–575.

[13] Chatterjee et al., "Planar FSS Based Dual-Band Wire Monopole Antenna for Multi-Directional Radiation With Diverse Beamwidths," IEEE Access, vol. 10, pp. 30 427–30 435, 2022, DOI: 10.1109/ACCESS.2022.3159337.

[14] N. Melouki, A. Hocini, and T. A. Denidni, "Performance enhancement of an ultra-wideband antenna using a compact topology optimized single frequency selective surface-layer as a reflector," Int. J. RF Microwave Comput.-Aided Eng., vol. 32, no. 5, 2022, e23097.

[15] Ud din, S. Ullah, and M. R. Akram, "UWB monopole antenna backed by single layer FSS for high gain antenna applications," in 2022 Workshop on Microwave Theory and Techniques in Wireless Communications (MTTW), IEEE, 2022, DOI: 10.1109/mttw56973.2022.9942622.

[16] P. Jha et al., "Super Ultra-Wideband Planar Antenna with Parasitic Notch and Frequency Selective Surface for Gain Enhancement," ACES Journal, 2022, pp. 757–764.

[17] Shi et al., "Gain Enhancement of a Dual-Band Antenna with the FSS," Electronics (Switzerland), vol. 11, no. 18, p. 2882, 2022, DOI: 10.3390/electronics11182882.

[18] S. Ali et al., "Measurement engineering to designatruncated ground plane compact circular ring monopole patch antenna for ultra wideband applications," Wireless Personal Communications, 2022, pp. 1–20.

[19] R. Sengupta et al., "FSS superstrate loaded SIW circular cavity-backed cross-shaped slot antenna for wireless applications," J. Electromagn. Waves Appl., vol. 36, no. 16, pp. 2271–2288, 2022, DOI: 10.1080/09205071.2022.2072239.

[20] Al-Gburi et al., "Compact size and high gain of CPW-fed UWB strawberry artistic shaped printed monopole antennas using FSS single layer reflector," IEEE Access, vol. 8, pp. 92 697–92 707, 2020.

[21] R. Mondal et al., "Compact ultra-wideband antenna: Improvement of gain and FBR across the entire bandwidth using FSS," IET Microwaves, Antennas and Propagation, vol. 14, no. 1, pp. 66–74, 2020, DOI: 10.1049/iet-map.2019.0536.

[22] S. Kundu, "A compact uniplanar ultra-wideband frequency selective surface for antenna gain improvement and ground penetrating radar application," Int. J. RF Microwave Comput.-Aided Eng., vol. 30, no. 10, 2020, e22363.

[23] Chatterjee et al., "Planar FSS Based Dual-Band Wire Monopole Antenna for Multi-Directional Radiation with Diverse Beamwidths," IEEE Access, vol. 10, pp. 30 427–30 435, 2022.

[24] R. Mondal et al., "Compact Ultra-Wideband Antenna: Improvement of Gain and FBR Across the Entire Bandwidth Using FSS," IET Microwaves, Antennas & Propagation, vol. 14, no. 1, pp. 66–74, 2020.

[25] S. Ullah and M. R. Akram, "UWB monopole antenna backed by single layer FSS for high gain antenna applications," in 2022 Workshop on Microwave Theory and Techniques in Wireless Communications (MTTW), IEEE, 2022.

[26] M. M. H. Mahfuz et al., "A Notched UWB Microstrip Patch Antenna for 5G Lower and FSS Bands," Microwave and Optical Technology Letters, vol. 64, no. 4, pp. 796–802, 2022.

Tamara Zuhair Fadhil received B.Sc. and MSc degree in Electrical and Electronic Engineering department from the University of Technology, Baghdad, Iraq. She is currently pursuing a Ph.D. degree in Electrical Engineering at Universiti Teknologi Malaysia. She has been a Lecturer at the University of Information Technology and Communications (UOITC), Baghdad, Iraq, since December 2016. Her current research interests include the design of multiple-beam metasurface Antenna systems for fifth-generation Applications.

Noor Asniza Murad (Senior Member, IEEE) obtained her first-degree Bachelor of Engineering (Electrical – Telecommunications) in 2001 from Universiti Teknologi Malaysia (UTM). Shortly after graduated, she served UTM as a tutor attached to the Department of Radio Communication Engineering (RaCED), Faculty of Electrical Engineering (FKE), UTM. She received her Master of Engineering (Electrical) in 2003 from the same university and been appointed as a lecturer in April 2003. She joined Emerging Device Technology Group, University of Birmingham, UK and obtained her Ph.D in 2011 for research on Micromachined Millimeterwave Circuits. She attached to HID GLOBAL Sdn Bhd for one year under Research and Development specifically working on RFID tag design, testing and development. Her research interests include antenna design for RF and microwave communication systems, millimeterwave circuits design, RFID and antenna beamforming. Currently, Noor Asniza Murad is a senior member of IEEE (MIEEE), MBOT Professional Technologist, and Associate Professor at the School of Electrical Engineering, Universiti Teknologi Malaysia (UTM).

M. R. Hamid received the M.Sc. degree in communication engineering from Universiti Teknologi Malaysia (UTM), Johor Bahru, Malaysia, in 2001 and the Ph.D. degree from the University of Birmingham, Birmingham, U.K., in 2011. He has been with the Faculty of Electrical Engineering (FKE), UTM, since 1999, where he is currently a senior lecturer. His major research interest includes reconfigurable antenna design for multimode wireless applications.